Selective photocurrent generation in HfO2 and carbon nanotube hybrid nanocomposites under Ultra-Violet and visible photoexcitations

P. Rauwel, Augustinas Galeckas, F. Ducroquet, E. Rauwel

Selective photocurrent generation in HfO_2-CNT hybrid nanocomposites under UV and visible photoexcitations

P. Rauwel,[1,2a] Augustinas Galeckas[3], F. Ducroquet[4] and E. Rauwel[1,2]

[1]*Department of Engineering, Tallinn University of Technology,*

Puistee 78, 51008 Tartu, Estonia

[2]*Estonian University of Life Science, Institute of Technology, Kreutzwaldi 56/1*

51014 Tartu, Estonia

[3]*Department of Physics, University of Oslo. P.O. Box 1048, Blindern, 0316 Oslo, Norway*

[4]*IMEP-LAHC, Minatec, 3 Parvis Louis Néel, University Grenoble Alpes, Grenoble, France*

[a]protima.rauwel@emu.ee

ABSTRACT

We report on the photocurrent generation in HfO_2-CNT nanocomposites under UV and visible excitations at zero bias. Cubic phase HfO_2 nanoparticles have been combined with multi-walled carbon nanotubes in this work. The cubic phase of HfO_2 has been stabilized by oxygen vacancies which act as luminescent band gap states. In a broad UV-visible range of below band gap photoexcitation, a photocurrent is generated which was found to be most efficient under UV illumination. We discuss the possible mechanism in terms of a CNT assisted charge transfer involving optically active surface states of the HfO_2 nanoparticles. The abrupt generation and relaxation responses of the photocurrent on/off cycles along with a constant steady state current as high as 200nA for 1mg of the nanocomposite, has potential in energy harvesting and other applications requiring stable charge retention.

KEYWORDS

Photocurrent, HfO_2, nanoparticles, Carbon nanotubes, hybrid nanocomposites, surface states

1. Introduction

Hybrid materials such as CNT decorated with metal oxide nanostructures offer various applications in fields such as catalysis,[1] optoelectronics,[2] photovoltaics[3,4], among many others.[5] The optical responsivity of CNT alone is very low and is therefore not suitable for optoelectronic or energy harvesting applications.[6] However, when combined with other photosensitive inorganic nanoparticles, it facilitates the transfer of charges from the nanoparticles[7] or chromophores owing to electrostatic band bending at the interfaces of such hybrid structures.

HfO_2 is a renowned dielectric material and the cubic phase of HfO_2 presents a higher dielectric constant than the stable monoclinic phase[8-1011,12]. Recently, the cubic phase of pure HfO_2 nanoparticles was stabilized without dopants, through the creation of oxygen vacancies via non

aqueous sol-gel routes.[13] Their photoluminescence emission in the visible region was attributed to the presence of oxygen vacancies and surface defects in these nanomaterials with average sizes of 2.5nm.[13] Another study revealed that the luminescence emission at 3.1eV of Hf^{3+} trap states was enhanced when HfO_2 was combined with CNT, ascertaining their participation in the generation of photocurrent.[14] We succinctly demonstrated the generation of a photocurrent only under UV excitation at zero bias.[15,16] In this Letter, we further illustrate that even a small amount of the HfO_2-CNT nanocomposite (~ 1 mg) spread over symmetrical copper electrodes, is capable of producing a photocurrent upon UV and visible photoexcitations at zero bias.

2. Materials and Methods

2.1 Synthesis

The procedure for synthesizing cubic phase HfO_2 NPs has been described elsewhere.[13] NANOCYL NC7000 MWCNTs with an average diameter and length of 10nm and 1.5μm, respectively, were purchased. The HfO_2 nanoparticles were dispersed in pure ethanol along with the MWCNTs and sonicated for 2 hours.

2.2 Characterization

High resolution transmission electron microscopy (HRTEM) was carried out on a Titan G2 80-200 microscope operating at 200 kV with a point-to-point resolution of 2.4Å. The electrical measurements were carried out using two source measure units (Agilent 4156). The sample was illuminated by a 125W Hg lamp emanating at wavelength of 365nm. For the visible excitation, the microscope light source integrated into the electrical measurement equipment was used, allowing illumination at two discrete spectral ranges, blue (475nm) and yellow (575nm).

3. Results and discussion

The TEM overview in figure 1(a) illustrates the intertwining of the CNT and the decoration of the HfO_2 on the CNT walls creating an intimate contact for an efficient transfer of charges. Figure 1(b) further illustrates two connecting nanotubes and HfO_2 nanoparticles on their surfaces.

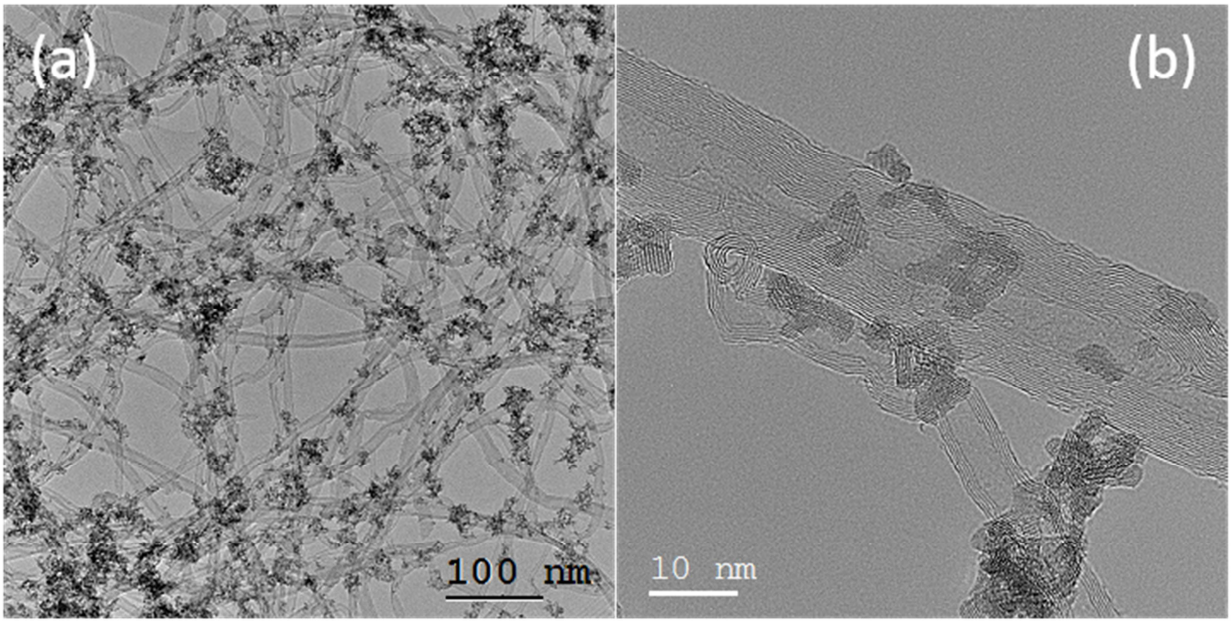

Fig. 1. TEM images of CNT-HfO_2 nanocomposites (a) over view (b) higher resolution.

The optical properties viz. diffuse reflectance and photoluminescence spectroscopies of the HfO_2-CNT hybrid nanocomposite have been studied earlier and are reported in detail elsewhere.[15] The MWCNT are metallic as reported in that study. The PL spectra obtained at room temperature under UV excitation of 325nm have revealed that the strongest emission at 3.1eV is associated to the Hf^{3+} surface states of the HfO_2 nanoparticles.[14] Other components centered within the 2-3eV range correspond to surface defects and/or impurities introduced during the synthesis of the nanocomposites and are most probably related to differently

coordinated oxygen vacancies.[17] In particular, the deep level trap at 2.5eV is related to oxygen vacancies (Vo), which are readily formed due to the large amounts of Hf^{3+} states. It is also noteworthy that the high surface-to-volume ratio of the HfO_2 nanoparticles of sizes as small as 2.6 nm (Fig. 1(b)), implies that most of the atoms are on the surface of the NPs and therefore, the surface states consist of both Hf^{3+} and Vo.[14] The CNT provide a conducting pathway for the trapped charges at these surface states, which is essential in the generation of photocurrent.[15]

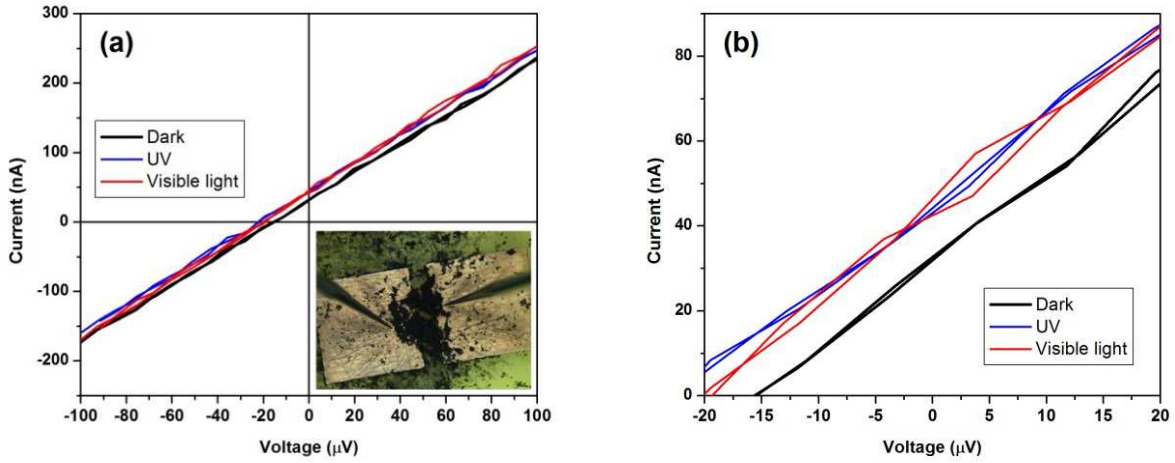

Fig. 2. (a) I-V curves of the sample under different illumination conditions: dark, UV and visible. Inset is the nanocomposite sample deposited between Cu electrodes for electrical measurements, (b) enlargement of figure 2(a) highlighting the current increase of 15nA under light excitation (high precision voltage source apparatus is not used in this experiment, which can explain the slight current offset observed under dark condition at 0Volt).

For I-V and photocurrent measurements, the nanocomposite was spread across two symmetrical copper electrodes of dimensions of 1cm × 1cm (inset figure 2(a)). The nanocomposite was first mixed in ethanol to make a homogeneous mixture. A droplet of this mixture was spread across the electrodes with a drying time of approximately 2 minutes between successive drops in order to have a flat sample without lumps. In all, 1mg of the nanocomposite was deposited between the

electrodes. The I-V measurements were carried out in the dark and also under UV and visible illuminations.[18] In all of these cases, the conduction was ohmic in the voltage range used. On illuminating with visible and UV lights, there was a 15nA increase in the current at 0V (fig.2(b)), implying an increase in minority carriers.[18]

In order to eliminate a possible heating effect by the excitation illumination, the current was measured under zero bias as well as 1mV for different temperatures without illumination. The measurements performed under zero bias show no noticeable temperature dependence with the current values within a range of 30-40nA (figure SI,1(a))). Under 1mV bias, a steady increase of the current by 30nA from its initial value can be observed in figure (figure SI, 1(b)). The current increase corresponds to a decrease of the resistance with the increase in temperature. When the temperature is stabilized at 80°C (t>300s), the current remains stable without any significant Joule heating effects. No current increase was observed under zero bias and the current increase of 30nA observed at 80ºC under 1mV is negligible compared to the current increase measured under photoexcitation. In addition, the local heating in the sample is most probably lower than 80ºC as opposed to the applied temperature.

Figure 3 demonstrates that the generated photocurrent depends on the spectral content of the illumination reaching a higher value under UV excitation. The UV source emits higher energy photons (3.3eV) compared to visible source (2.6 and 2.25eV, respectively). It is noteworthy that in all the cases only the mid-band gap states could be excited considering the wide band gap of HfO_2 of 5.7eV. However, other factors such as the density and absorption cross-sections of the defect states in the NPs, as well as the actual energy flux emitted from the different illumination sources are all critical in the generation of the photocurrent. The ultimate photocurrent is also

dependent on the density of the probed nanocomposites and on the distance between the electrodes.

Various on/off cycles for the nanocomposites that were homogeneously dispersed between the two symmetrical copper electrodes, were studied under both illuminations figures 3(a) and (b). For longer cycles of 20s a steady state current is observed under UV illumination, while as a dip in the current is observed when illuminated with visible light once maximum photocurrent is reached. For shorter on/off cycles the photocurrent on UV excitation tends to produce a photocurrent with the same reliability. On the other hand, under visible illumination, for all the on/off illuminations shown in figure 3(b), the response time to photo-excitation is delayed compared to under UV excitation.

A two-step increase in photocurrent is observed when excitation is turned on in figure 3(c). Under UV illumination a prompt onset followed by an exponential increase of the photocurrent in a first step (up to 'τ_1' in the figure) is observed followed by a slower rise at up to 'τ3' of illumination before attaining a steady state. The exponential increase implies a rapid increase of excitons bound to various trap states that are quickly discharged via the CNT. However, as and when these trap states start reaching their maximum capacity the photocurrent increase is less prominent. A stable photocurrent is observed, suggesting that an equilibrium of charges in the trap states has been attained. Similarly, in the off state a similar two-step decrease is observed, first an exponential decrease followed by a slower one until reaching the off state. However, under visible illumination, in the on-cycle firstly, the rapid exponential increase is not observed. A one-step gradual increase in the photocurrent up to τ_2 of illumination, followed by an almost

stable current at τ_3, beyond which a slight and gradual decrease in the current, are observed. The off-cycle manifests a similar trend with a two-step (τ_4) gradual decrease of the photocurrent.

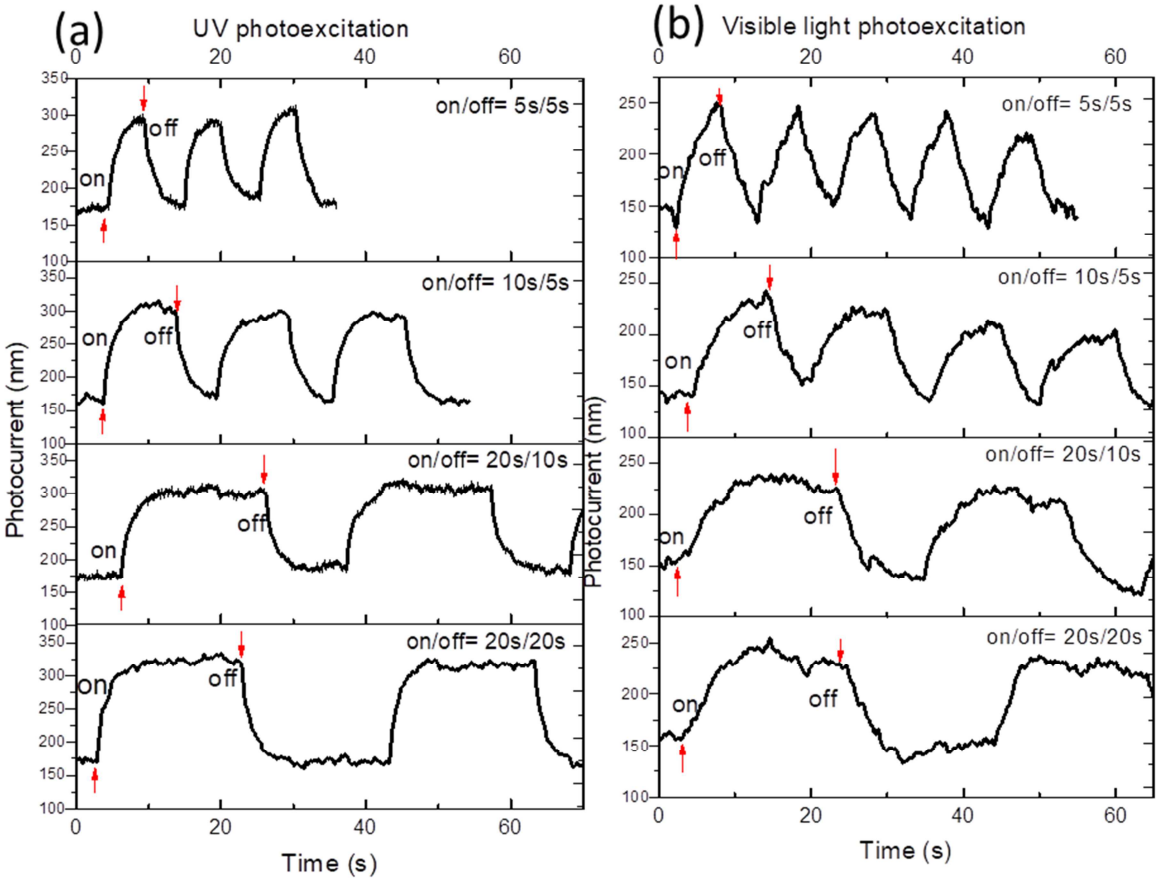

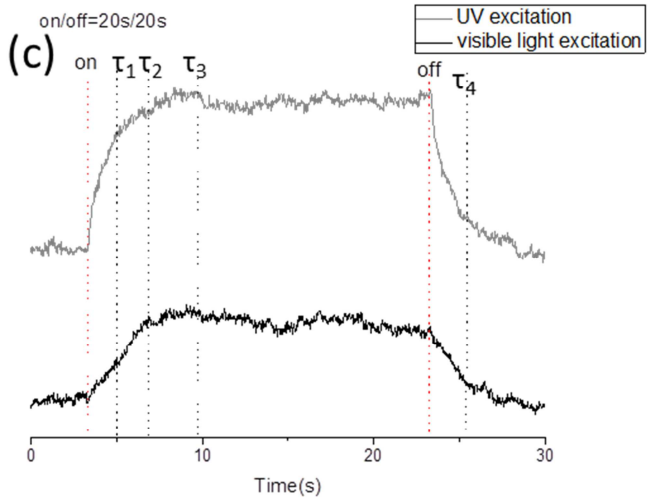

Fig. 3. Current *vs* time characteristics of the HfO_2-CNT nanocomposite at various on-off times under (a) UV, (b) visible light illuminations and (c) comparison of the photocurrent under the 2 illuminations with on/off=20s/20s under zero bias.

Under UV excitation, photogenerated carriers are transferred to the Hf^{3+} states at the surfaces of the nanoparticles. These surface states could also harbor C atoms of the CNT, which in turn creates band bending and facilitating charge transfer. With regards to photoexcitation under visible light, the photon energy of ~2.6eV is able to excite carriers only to oxygen vacancy related band gap states which tend to emanate between 2-2.6eV.[14] This implies that the Hf^{3+} states do not participate in the photocurrent generation when excited in the visible, as they are only excitable by higher photon energies like UV. In addition, a lower photon energy excitation source would also decrease the overall number of excitons generated and would be one of the factors responsible in producing a lower photocurrent. This however does not degrade the optical quality of the material and several successive experiments have shown recovery of the original properties when the on-off cycle time and illumination changed.

Moreover, the two tendencies in the photocurrent profiles under the two excitations also suggest that different surface states participate in the photocurrent generation. Hf^{3+} states excited by UV illumination tend to have a faster response time along with a higher stability and a more efficient charge transfer than the differently coordinated Vo. In addition, we have observed that the time response is rapid compared to some other nanomaterials.[19,20] A maximum photocurrent of 200nA was measured for a small quantity of HfO_2-CNTs hybrid nanocomposite, which makes this new generation nanocomposite a promising candidate for photocurrent production as even visible light photoexcitation produces a photocurrent.

4. Conclusion

In this work, we have synthesized a nanocomposite of HfO_2-CNT that shows unique photocurrent generation properties under UV and visible light excitations. For 1mg of nanocomposite, the photocurrent on UV excitation is around 100nA higher than under visible excitation mostly due to higher energy photons available for UV excitation. Efficiency of photocurrent generation by varying nanocomposite quantities is underway.

ACKNOWNLEDGEMENTS

This research was supported by the ERDF project EQUITANT (TK134/F180175TIBT), Estonian Research Council (grant PUT431), Research Council of Norway and the University of Oslo through the FUNDAMENT project (No. 251131).

REFERENCES

1 F. Ye, X. Cao, L. Yu, S. Chen, and W. Lin, Int. J. Electrochem. Sci **7,** 1251 (2012).
2 E. Rauwel, A. Galeckas, M. R. Soares, and P. Rauwel, The Journal of Physical Chemistry C **121,** 14879 (2017).
3 P. V. Kamat, The Journal of Physical Chemistry C **112,** 18737 (2008).
4 S. Y. Jeong, S. C. Lim, D. J. Bae, Y. H. Lee, H. J. Shin, S.-M. Yoon, J. Y. Choi, O. H. Cha, M. S. Jeong, D. Perello, and M. Yun, Applied Physics Letters **92,** 243103 (2008).
5 B. I. Kharisov, O. V. Kharissova, U. Ortiz Méndez, and I. G. De La Fuente, Synthesis and Reactivity in Inorganic, Metal-Organic, and Nano-Metal Chemistry **46,** 55 (2016).
6 P. Rauwel, M. Salumaa, A. Aasna, A. Galeckas, and E. Rauwel, Journal of Nanomaterials **2016,** Article ID 5320625 (2016).
7 F. Li, H. Wang, D. Kufer, L. Liang, W. Yu, E. Alarousu, C. Ma, Y. Li, Z. Liu, C. Liu, N. Wei, F. Wang, L. Chen, O. F. Mohammed, A. Fratalocchi, X. Liu, G. Konstantatos, and T. Wu, Advanced Materials **29,** 1602432 (2017).
8 J. Robertson, Reports on Progress in Physics **69,** 327 (2006).
9 C. Dubourdieu, E. Rauwel, C. Millon, P. Chaudouët, F. Ducroquet, N. Rochat, S. Rushworth, and V. Cosnier, Chemical Vapor Deposition **12,** 187 (2006).
10 J. H. Choi, Y. Mao, and J. P. Chang, Materials Science and Engineering: R: Reports **72,** 97 (2011).
11 E. Rauwel, C. Dubourdieu, B. Holländer, N. Rochat, F. Ducroquet, M. D. Rossell, G. V. Tendeloo, and B. Pelissier, Applied Physics Letters **89,** 012902 (2006).
12 C. Dubourdieu, E. Rauwel, H. Roussel, F. Ducroquet, B. Holländer, M. Rossell, G. V. Tendeloo, S. Lhostis, and S. Rushworth, Journal of Vacuum Science & Technology A **27,** 503 (2009).
13 P. Rauwel, E. Rauwel, C. Persson, M. F. Sunding, and A. Galeckas, Journal of Applied Physics **112,** 104107 (2012).

14 E. Rauwel, A. Galeckas, and P. Rauwel, Materials Research Express **1,** 015035 (2014).
15 P. Rauwel, A. Galeckas, M. Salumaa, F. Ducroquet, and E. Rauwel, Beilstein Journal of Nanotechnology **7,** 1075 (2016).
16 P. Rauwel, A. Galeckas, M. Salumaa, A. Aasna, F. Ducroquet, and E. Rauwel, IOP Conference Series: Materials Science and Engineering **175,** 012064 (2017).
17 J. L. Gavartin, D. M. Ramo, A. L. Shluger, G. Bersuker, and B. H. Lee, Applied Physics Letters **89,** 082908 (2006).
18 J. Reemts and A. Kittel, Journal of Applied Physics **101,** 013709 (2007).
19 Z. Jin and J. Wang, Journal of Materials Chemistry C **2,** 1966 (2014).
20 Y. Lee, J. Yang, D. Lee, Y.-H. Kim, J.-H. Park, H. Kim, and J. H. Cho, Nanoscale **8,** 9193 (2016).